Impact of future climate change on water supply and irrigation demand in a small mediterranean catchment. Case study: Nebhana dam system, Tunisia

M. Allani, R. Mezzi, A. Zouabi, R. Béji, F. Joumade-Mansouri, M. E. Hamza and A. Sahli

ABSTRACT

This study evaluates the impacts of climate change on water supply and demand of the Nebhana dam system. Future climate change scenarios were obtained from five general circulation models (GCMs) of CMIP5 under RCP 4.5 and 8.5 emission scenarios for the time periods, 2021–2040, 2041–2060 and 2061–2080. Statistical downscaling was applied using LARS-WG. The GR2M hydrological model was calibrated, validated and used as input to the WEAP model to assess future water availability. Expected crop growth cycle lengths were estimated using a growing degree days model. By means of the WEAP-MABIA method, projected crop and irrigation water requirements were estimated. Results show an average increase in annual ETo of 6.1% and a decrease in annual rainfall of 11.4%, leading to a 24% decrease in inflow. Also, crops' growing cycles will decrease from 5.4% for wheat to 31% for citrus trees. The same tendency is observed for ETc. Concerning irrigation requirement, variations are more moderated depending on RCPs and time periods, and is explained by rainfall and crop cycle duration variations. As for demand and supply, results currently show that supply does not meet the system demand. Climate change could worsen the situation unless better planning of water surface use is done.

Key words | downscaling, GR2M, hydrological modelling, irrigation water requirement, water supply and demand, WEAP-MABIA

M. Allani (corresponding author)
R. Mezzi
A. Sahli
Laboratoire des Sciences Horticoles (LSH), Institut National Agronomique de Tunisie (INAT),
Université de Carthage (UC),
43, Avenue Charles Nicolle 1082,
Tunis-Mahrajène,
Tunisia
E-mail: *mohamed.allani@gmail.com*

A. Zouabi
R. Béji
F. Joumade-Mansouri
Commissariat Régional au Développement Agricole de Kairouan (CRDA),
Cité Sidi Layoun, Kairouan 3100,
Tunisia

M. E. Hamza
Institution de la Recherche et de l'Enseignement Supérieur Agricoles (IRESA),
30, Rue Alain Savary 1002, Tunis Belvédère,
Tunisia

INTRODUCTION

A combination of climate change and increase in irrigation usage is likely to substantially decrease fresh water availability (by 2–15% for 2 °C of warming), especially in Mediterranean regions, which would lead to the largest decreases in the world (Cramer *et al.* 2018). In fact, these regions are likely to warm at a rate about 20% greater than the global annual mean surface temperature (Lionello & Scarascia 2018). For these countries, water management is facing major challenges due to increasing uncertainties caused by climate change. Policies need to mitigate these risks and consider adaptation options; however, decision-makers currently lack adequate information, particularly in the south Mediterranean regions where impact assessment studies are limited (Cramer *et al.* 2018).

In these regions, the use of water management tools, taking into consideration water supply and demand variability in an integrated way, are needed. Water Evaluation and Planning software (WEAP) is a modelling decision support system that helps assess climate, hydrology, land use, infrastructure and management priorities at regional levels

doi: 10.2166/wcc.2019.131

(Yates *et al.* 2005a, 2005b). WEAP has been widely used around the world with differents objectives, such as the management of surface and groundwater resources, adaptation strategies and policy changes.

Adgolign *et al.* (2016) used WEAP to model the surface water resources allocation of Didessa sub-basin in West Ethiopia. WEAP was used by Psomas *et al.* (2016) to design water efficiency measures in the basin of Ali Efenti in Greece. Hamlat *et al.* (2013) used WEAP to evaluate and analyse the existing balance and expected future water resources management scenarios in western watersheds of Algeria by taking into account the different operating policies and factors that may affect demand in the region. Finally, Höllermann *et al.* (2010) used WEAP to assess future water situations under different scenarios of socio-economic development and climate change affecting the Ouémé Basin in Benin.

Studies that cover climate change impact assessment at local scale require downscaling of coarse general circulation model (GCM) projections to a high resolution scale that can characterize a representative situation. Two types of downscaling can be used, namely, statistical and dynamical downscaling. While dynamical downscaling is based on a regional climate model (RCM), which is costly and constrained by the resolution of the RCM, statistical downscaling applies statistical links between large-scale GCM and local observations (Olsson *et al.* (2017). Dynamical downscaling and statistical downscaling approaches have their own advantages and disadvantages, but there is no consensus that one approach is superior in terms of reproducing the observed variability of local climates (Salehnia *et al.* 2019). Statistical downscaling can be divided into three most commonly used approaches, which are transfer functions, weather typing and stochastic weather generator. Various statistical and dynamical downscaling have been applied in different studies regarding expected future climate impact on temperature and precipitation (Teutschbein & Seibert 2012; Chen *et al.* 2013; Hassan *et al.* 2014; Nguyen *et al.* 2017; Fenta Mekonnen & Disse 2018; Ishida *et al.* 2018), hydrological modelling (Okkan & Fistikoglu 2014; Ouyang *et al.* 2015; Lee & Bae 2016; Al-Safi & Sarukkalige 2017) or crop growth modelling (Schlenker *et al.* 2007; Acharjee *et al.* 2017; Liu *et al.* 2017). The use of an ensemble of GCM models instead of individual models, when applying downscaling method, can reduce the uncertainties introduced by the GCMs and the possibility of misleading assessment of climate change impacts, thus giving better simulation of the climate conditions (Liu *et al.* 2017; Reshmidevi *et al.* 2018). In this study, as one statistical downscaling method, a stochastic weather generator, namely, LARS-WG 6.0 (Semenov *et al.* 1998; Semenov & Barrow 2002), was used to extract the local-scale future daily rainfall temperature and radiation from five GCMs of the CMIP5 available in the software incorporating the daily observed climate data under two representative concentration pathways (RCPs) (4.5 and 8.5). The LARS-WG weather generator has been widely used in impact assessment studies because it is not only computationally inexpensive, it delivers climate scenarios that match the statistical properties of observed weather and provide daily meteorological variables while preserving statistical interrelationships between variables (Semenov & Stratonovitch 2015). All climatic models' outputs involve a number of biases that, if not corrected, can lead to significant errors in impact assessments. Therefore, bias correction of models' outputs is necessary before their use in impact analyses (Ahmed *et al.* 2013; Cannon *et al.* 2015; Nguyen *et al.* 2017). As described by Semenov & Stratonovitch (2015), LARS-WG 6.0 version integrates a series of steps to bias correct GCM outputs when generating climatic data under the CMPI5.

Hydrological modelling is essential for water resources management and impact studies. In the literature, two different approaches are proposed to simulate climate change impact on hydrological regimes. The first one is based on the direct use of runoff simulated by GCMs from the CMIP5 (Alkama *et al.* 2013; Freedman *et al.* 2014; Zheng *et al.* 2018). The second commonly used approach suggests the use of calibrated hydrological models to better understand the hydrological process in impact studies. Moreover, in the hydrological modelling research, physically based distributed models such as the Soil and Water Assessment Tool (SWAT) (Sellami *et al.* 2016; Rouhani & Jafarzadeh 2017; Abeysingha *et al.* 2018) and conceptual lumped models such as HBV and BTOPMC models (Phan *et al.* 2010; Todorovic & Plavsic 2016; Al-Safi *et al.* 2020) are proposed. Also, as highlighted by Al-Safi *et al.* (2020), there is a continuing debate in the hydrologic modelling research area on whether physically based distributed

models better capture recorded streamflow than the conceptual lumped models approach does. Therefore, a better understanding of the hydrological processes in impact studies should not necessarily translate into the use of more complex models (Blöschl & Montanari 2010). Lumped models are the most widely used tools for operational applications because they offer simplified catchment-scale representations of the precipitation's transformation into river discharge (Coron *et al.* 2017). When dealing with climate change impact on water supply and demand systems and the general evolution of the overall water availability, the use of monthly time step hydrological models is accepted (Lespinas *et al.* 2014). In this study, the GR2M model (*Génie Rural à 2 paramètres au pas de temps Mensuel*), a parametric conceptual hydrological model, was chosen because it performed well for the assessment of the impacts of climate change on runoff (Zeroual *et al.* 2013; Okkan & Fistikoglu 2014; Sellami *et al.* 2016).

The response of agricultural systems to climate change will depend on management practices, especially the availability and levels of applied water. The most affected aspects for crops refer to the changes of phenological dates, length of growing season, crop water requirement and irrigation water requirement (Saadi *et al.* 2015). A warmer climate may increase the reference evapotranspiration (ETo) of crops leading to greater demand for irrigation, and consequently higher ETc. However, a change in air temperature may also alter the length of crop growing period (Chattaraj *et al.* 2014). Assessing climate change impact of a water supply and demand system requires the study of the impact of climate change on crops. Luo *et al.* (2015) evaluated changes in water requirements for several crops like wheat, maize, cotton, millet and soybean under climate change in the North China plain, and Chowdhury *et al.* (2016) on wheat, maize, barley, tomato, potato, other vegetables, clover, date, citrus and grapes in Saudi Arabia. Both studies were done without considering the impact of change in temperature on crops' growing periods. On the other hand, studies have tended to focus on single crops, taking into consideration the phenological effect when dealing with climate change impact, such as Knezevic *et al.* (2017) for olive trees in Montenegro, Han *et al.* (2017) and Ahmad *et al.* (2019) on wheat crop in the Heihe river basin, China and Punjab, Pakistan, respectively, and finally Pathak & Stoddard (2018) on tomato in California.

The specific objectives of this research are to: (1) analyse the impact of climate change on rainfall and reference evapotranspiration; (2) evaluate the variability of the water supply to a system through the inflow received to a reservoir; (3) study the impact of climate change on crop growth cycle; (4) calculate crop water demand and irrigation water demand; (5) examine the expected future change in irrigation demand of the whole system.

STUDY AREA

The study area, referred to as the Nebhana dam system, is located in the centre of Tunisia, downstream of the Nebhana watershed, and is composed of six public irrigated districts (Figure 1). The reservoir is supplied by two main rivers, Maarouf and Nebhana. Through a system of pipelines, water is delivered to supply the six irrigated districts within the study area and also for irrigation and domestic use outside the watershed.

The Nebhana dam system has semi-arid weather with a cool wet season from November to March and a dry hot season from May to September. The average annual rainfall (1985–2004) is 309 mm and the reference evapotranspiration (1985–2004) is 1,327 mm.

The six irrigated districts occupy an area of 2,068 ha and are Ain Boumorra 1, 2 and 3, Fadhloun, Dar Jameya and Sisseb 1. Ain Boumorra 1, 2 and 3 and Fadhloun were created in 1973 as the only areas irrigated from the Nebhana dam in the region. Later on, the irrigated districts Dar Jameya and Sisseb 1 were connected to the pipeline in response to the groundwater depletion, in 2002 and 2008, respectively. Concerning water resources management, the pipeline is managed by the Société d'Exploitation du Canal et Adductions des Eaux du Nord (SECADENORD), and is in charge of providing water from the dam. At the level of each irrigated district, a water users' association is responsible for the distribution, billing and maintenance of the network. When created, the main land use of the irrigated districts Ain Boumorra 1, 2, 3 and Fadhloun was exclusively fruit trees with mainly apricot, citrus and olive trees. Vegetables (mainly green peas and pepper) and

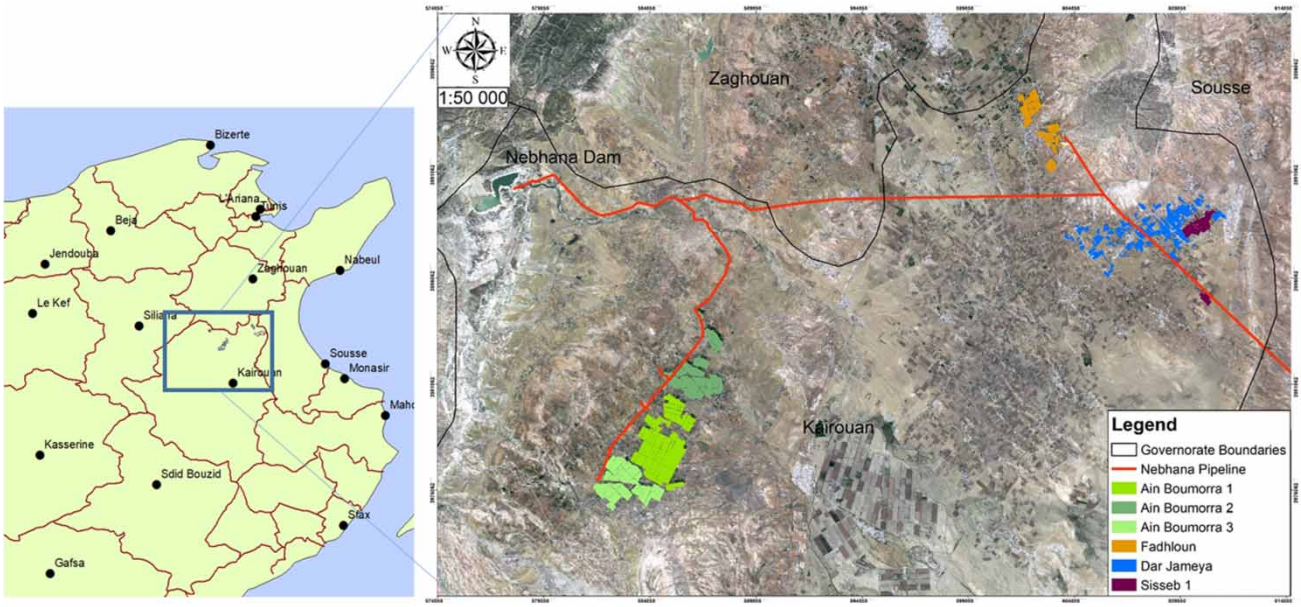

Figure 1 | Location map of the study area showing the Nebhana dam, the water network and the irrigated districts.

cereals, were then integrated into the cropping system. The irrigated districts of Dar Jameya and Sisseb 1 have a more diverse land use with a mixture of fruit trees (mainly olive and pomegranate), cereals and vegetables. Regarding water usage, the Nebhana dam system uses an average of 4,600 m^3/ha. However, the irrigated districts of Ain Boumorra 1, 2 and 3 as well as Fadhloun present a high annual consumption of 5,400 and 5,100 m^3/ha/year, respectively, whereas Dar Jameya and Sisseb only use 2,400 and 2,700 m^3/ha/year.

METHODS

Data collection and characterization of the study area

The collected data were relative to irrigation and crop water requirements. They focused on climatic data, land use and cultivated area, crop and soil characteristics and volume of supplied water to the Nebhana dam system.

Climate characterization

Daily meteorological data were obtained from the Tunisian National Institute of Meteorology (INM) from Kairouan climatic station located 30 km from the study area. The climate data include maximum temperature (T_{max}, °C), minimum temperature (T_{min}, °C), maximum relative humidity (RH_{max}, %), minimum relative humidity (RH_{min}, %), sunshine duration (SD, hrs) and wind speed (U_2, m/s). Daily rainfall (P, mm) data were collected from a rain gauge located within the study area in a radius of 20 km from the farthest irrigated district. These data were obtained for the 1985–2004 period. Based on the collected data, the reference evapotranspiration (ETo) was calculated using the Penman–Monteith FAO 56 method (Allen *et al.* 1998).

Figure 2 presents the monthly average rainfall and ETo of the study area based on the data for the 1985–2004 period. Rainfall is always lower than ETo, even in the rainiest month of September, where the average rainfall reaches 58 mm for an average ETo of 128 mm. Thus, the study area is always under climate deficit and changes of climate conditions could severely influence irrigation practices.

Water supply to the Nebhana dam system

Historical data concerning the dam operation were collected from the Direction Générale Des Barrages et des Grands Travaux Hydrauliques (DGBGTH) from the period

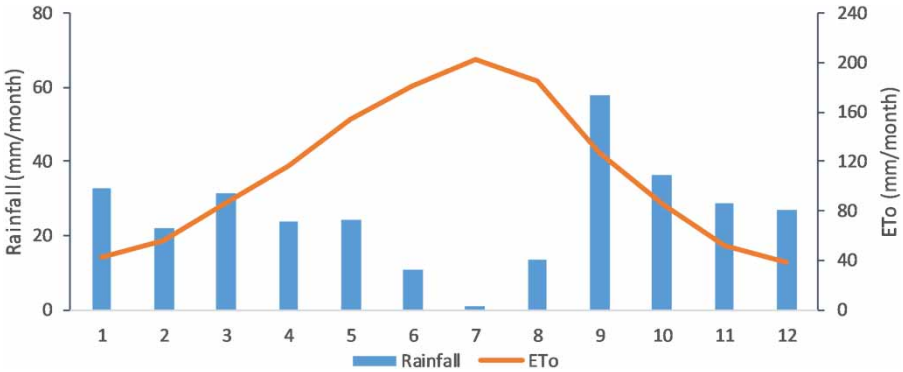

Figure 2 | Monthly average of ETo and rainfall.

of its commissioning, 1967 to 2017. The monthly average inflow and outflow of the Nebhana dam are plotted in Figure 3. The average annual inflow is 23.4 Mm^3 $year^{-1}$ with the lowest inflow reached during July and the highest inflow during March with 0.4 and 3.6 Mm^3 $month^{-1}$, respectively. Meanwhile, the average annual outflow from the dam is 21.3 Mm^3 $year^{-1}$. Since the primary use of the Nebhana dam is irrigation, outflow from the dam has the higher value during spring and summer with a maximum of 2.6 Mm^3 achieved during July. This is a critical issue for the study area where the Nebhana dam system barely ensures the balance between demand and supply.

Land use characteristics

Land use and land cover patterns in a region are the prerequisites for planning and implementing effective land use policies and schemes for sustainable regional development (Abdal & Suleiman 2004). In order to assess climate change impact on the water resources of the system, a field survey was performed during growing seasons 2014/2015, 2015/2016 and 2016/2017 to establish land use maps of the irrigated districts integrated in a geographic information system (GIS) database (Allani *et al.* 2018). These GIS data were used in defining and characterizing the current situation of land use in each irrigated district (Figure 4).

For the irrigated district Ain Boumorra 1, apricot, olive, citrus and green peas are the main crops with an area of 225.5, 161.4, 81.1 and 75.4 ha, respectively. In the irrigated district Ain Boumorra 2, citrus trees are the main crop and occupy 121.4 ha. Apricot and olive trees are also dominant crops with an area of 98.1 and 58.9 ha, respectively.

In the irrigated district Ain Boumorra 3, olive and apricot are the main crops with 122.4 and 125.9 ha. Green peas are also important crops with 65.5 ha. At the level of the irrigated district Fadhloun, olive trees are the main crop with an area of 89.4 ha representing 50% of the total area. The rest of the land is distributed between vegetables,

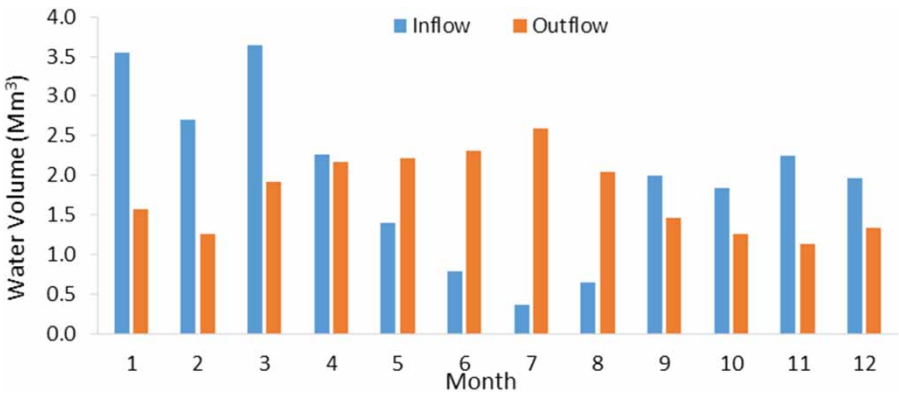

Figure 3 | Monthly average of inflow and outflow from the Nebhana dam.

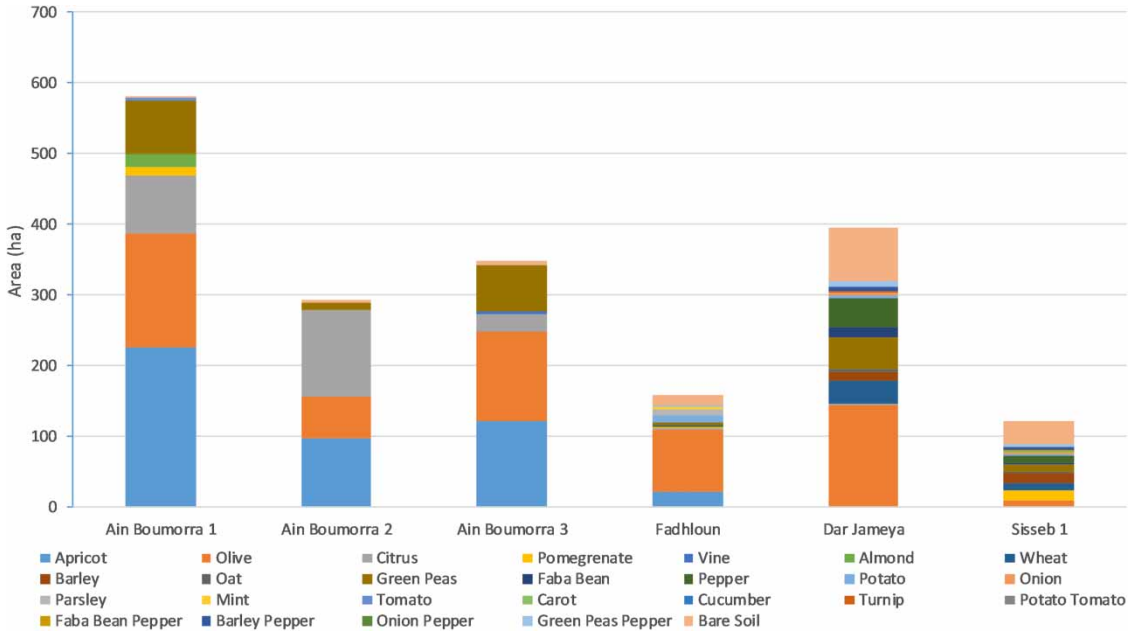

Figure 4 | Average land use of the six irrigated districts.

mainly potato, parsley, mint and green peas. In the irrigated district Dar Jameya, apart from olive trees which represent 144.7 ha, land use is more diversified. Vegetables occupied 124.4 ha, mainly green peas with 52.3 ha, pepper with 56.6 ha and faba beans with 14.7 ha. The remaining cropped vegetables are potato, tomato, onion, carrot and turnip. Cereals are also grown, but only representing 34 ha for wheat and 12 ha for barley, respectively. Finally, in the irrigated district Sisseb 1, pomegranate is the main fruit tree with an area of 13.8 ha, followed by olive with 9.2 ha. Cereals represent 30.6 ha of the land use, distributed between oat, barley and wheat. Vegetables are also cropped and use 37.8 ha.

Crop characteristics of the study area

To model crop water requirement (ETc) based on the FAO 56 method, crop characteristics are required (Allen *et al.* 1998). A monthly field survey was done on 400 plots during the growing season 2016/2017 to obtain information regarding planting date or bud burst, duration of each development stage, maximum height and rooting depth. Crop coefficients as well as depletion factor were obtained from the FAO 56 database (Table 1).

It is important to note that the created crop characteristics' database was validated during workshop sessions with the participation of stakeholders from all levels, including farmers as well as engineers from the local extension service and regional representatives of the ministry of agriculture.

Planting and bud burst (for tree crops) date was fixed to a single date for each crop (Table 1). Based on the actual length cycle of the studied crop, the daily growing degree days (GDD) was calculated over historical T_{max} and T_{min} (1985–2004) to obtain the average required GDD for each growing stage and crop cycle. The following GDD model was used:

$$GDD = \frac{T_{max} + T_{min}}{2} - T_{base}$$

where T_{base} is crop base temperature.

Soil characteristics

The soil water content at saturation, field capacity and wilting point are used to calculate soil water holding capacity. When missing, they can be estimated using pedotransfer functions and soil texture characteristics (Jabloun & Sahli 2006; McNeill *et al.* 2018). In our case, mean particle size

Table 1 | Crop characteristics' database of the study area

Crop	Apricot	Citrus	Pomegranate	Olive	Almond tree	Pepper	Tomato	Faba bean	Green peas AB	Green peas Sisseb	Cucumber	Potato	Onion	Oat	Wheat	Barley
Planting date/bud burst	05/03	25/02	01/03	05/03	15/02	20/04	10/03	01/11	01/09	15/10	15/03	15/02	01/09	15/12	15/12	20/11
Stage length initial [days]	30	90	70	30	30	45	20	30	32	32	15	25	20	35	35	35
Stage length dev [days]	50	30	35	75	35	40	30	30	45	45	25	25	45	50	40	45
Stage length mid-season [days]	130	150	70	75	140	100	30	60	65	65	30	31	20	50	75	60
Stage length end-season [days]	30	90	100	90	100	30	10	40	30	30	10	13	10	35	30	35
Stage length total [days]	240	360	275	270	305	215	90	160	172	172	80	94	95	170	180	175
T_{base} (°C)	6	12.8	10	15	4	10	10	4	4.4	4.4	12.8	2	0	2	0	2,970
Average cumulated GDD (°C)	4,204	2,893	3,570	2,243	5,507	3,229	847	1,579	2,266	1,805	525	1,422	2,066	2,372	2,970	2,245
Kcb: initial	0.6	0.75	0.4	0.385	0.2	0.15	0.15	0.15	0.15	0.15	0.15	0.15	0.15	0.15	0.15	0.15
Kcb: mid-season	0.8	0.7	0.8	0.45	0.85	1	1.1	1	1.1	1.1	0.95	1.1	0.90	1.1	1.1	1.1
Kcb: end	0.6	0.75	0.8	0.45	0.6	0.8	0.7	0.8	1.05	1.05	0.7	0.65	0.9	0.15	0.15	0.15
Depletion factor p	0.5	0.4	0.5	0.7	0.4	0.3	0.4	0.45	0.35	0.35	0.5	0.35	0.3	0.55	0.55	0.55
Height max [m]	4	4	2.5	4.5	4	0.7	0.65	1	0.6	0.6	0.3	0.6	0.4	0.9	0.9	0.9
Rooting depth [m] min	1.2	1.2	1.2	1.2	1.2	0.15	0.15	0.15	0.15	0.15	0.15	0.15	0.15	0.15	0.15	0.15
Rooting depth [m] max	1.2	1.2	1.2	1.2	1.2	0.75	1	0.6	0.8	0.8	0.70	0.5	0.45	1	1	1

at the level of each irrigated district was extracted from the Africa Soil Map database (van Engelen *et al.* 2005). Then, using a pedotranfer function developed by Jabloun & Sahli (2006) for Tunisian soils, characteristic soil water content was obtained (Table 2).

Hydrological model and inflow assessment: GR2M model

In order to simulate the sustainability of the Nebhana dam system, the GR2M hydrological model was used to simulate the stream inflow to the dam.

The GR2M is a conceptual rainfall-flow model that only requires monthly values of precipitation and potential evapotranspiration averaged over the drainage basins of interest. Rainfall data were estimated from the deterministic Thiessen interpolation method using QGIS© from two rain gauge stations located on the upper part of the Nebhana watershed and one at the level of the dam.

The structure of the GR2M is well described in Mouelhi *et al.* (2006). The model uses a spatial, temporal and conceptual lumping of hydro meteorological processes (Lespinas *et al.* 2014) and has two parameters, X1 and X2. Parameter X1 governs the soil moisture accounting, and X2 is used for calculating the groundwater exchange. Both parameters are optimized during model calibration. The GR2M has shown good results in different catchments in the Mediterranean region (Lespinas *et al.* 2014), Algeria (Bachir *et al.* 2015), China (Bai *et al.* 2015) and the U.S. (Ahn & Merwade 2014; Rungee & Kim 2017).

The model was calibrated and validated against natural inflow to the Nebhana dam using the AirGR package (Coron *et al.* 2017). Concerning data allocation, the temporal split approach, which is the most commonly used application of single-site comparison data for calibration/validation method, was applied (Daggupati *et al.* 2015). Bottcher *et al.* (2012) recommended using no more than one-third of the dataset for the model calibration, and at least two-thirds for validation was followed for data split. Thus, in this study, calibration was done for the period of 1985–1989 and evaluation for the period of 1990–2004.

One objective function was used to calibrate the GR2M model and two criteria were used to assess its efficiency, both for the calibration and validation periods. The objective function used for the calibration is the Nash–Sutcliffe efficiency (NSE) criterion calculated on square root transformed discharge where the criterion value has to be maximized (Nash & Sutcliffe 1970).

$$NSE\left(\sqrt{Q}\right) = 1 - \frac{\sum_i \left(\sqrt{Q_{obs,i}} - \sqrt{Q_{sim,i}}\right)^2}{\sum_i \left(\sqrt{Q_{obs,i}} - \sqrt{Q_{obs}}\right)^2}$$

where $\sqrt{Q_{obs,i}}$ represents the observed discharge on month i and $\sqrt{Q_{sim,i}}$ represents the simulated discharge on month i and $\sqrt{Q_{obs}}$ the mean of square root transformed observed discharge over the calibration period. NSE($\sqrt{Q}$) values vary from $-\infty$ and 1 for perfect simulation. It quantifies the ability of the model to explain discharge variability (Lespinas *et al.* 2014). As in different studies, the transformed NSE was used instead of the classical NSE because it gives a balanced image of the overall hydrograph fit and produces more all-purpose criteria (Oudin *et al.* 2006).

In addition to the transformed NSE, the model mean cumulative error (*CE*) was also used to assess its efficiency:

$$CE = 100\left(\frac{\sum_i Q_{sim,i}}{\sum_i Q_{obs,i}}\right)$$

where *CE* measures the ability of the model to correctly reproduce the total water volume observed over the simulation period. When it equals 100%, the water balance is perfectly simulated and when greater or lower than 100% it is overestimated or underestimated, respectively.

The obtained values X1 and X2 for the GR2M model are 10.341 for X1 and 0.200 for X2, respectively. Table 3 presents the performance of the model for the calibration and the validation periods.

Table 2 | Characteristic soil water content of the irrigated districts

Texture class	θ_{SAT} (%)	θ_{FC} (%)	θ_{WP} (%)	Available water capacity (%)
Ain Boumorra 1	42.51	29.07	9.69	19.38
Ain Boumorra 2	43.63	30.53	11.31	19.22
Ain Boumorra 3	52.46	29.41	9.98	19.43
Dar Jameya	43.60	31.82	12.21	19.61
Fadhloun	43.69	32.11	12.67	19.44
Sisseb 1	43.82	32.23	13.06	19.17

Table 3 | Performance of the GR2M model on the Nebhana dam

Criteria	Calibration period 1986–1989	Validation period 1990–2004
Nash$\sqrt{(Q)}$	0.62	0.63
CE (%)	78.30	108.06

Despite its simple structure, the calibrated GR2M model gave good results. The NSE$\sqrt{(Q)}$ values show that the monthly simulation of the inflow is satisfactory since it is greater than 0.5, as reported in Ahn & Merwade (2014). The average NSE$\sqrt{(Q)}$ for the whole period is 0.63. Regarding the CE criterion, the simulated inflow was underestimated during the calibration period and overestimated during the validation period with an average of 103.53% for the whole period. Figure 5 shows the modelled and observed runoff series of the calibration and validation periods.

Crop and irrigation water requirements for agricultural water demand: WEAP-MABIA method

Within WEAP, the MABIA method allows modelling of the soil water budget on a daily basis and the calculation of crop water requirement (ETc) as well as irrigation water requirement (IWR). It uses the dual crop coefficient (K_c) method of the FAO Irrigation and Drainage Paper No. 56 (Allen *et al.* 1998). It also allows the simulation of irrigation demand under different agricultural practices. The MABIA method includes modules that allow the estimations of the ETo based on available climatic data and soil water characteristics using pedotransfer methods (Jabloun & Sahli 2012).

The MABIA method has been used by different authors such as Esteve *et al.* (2015) and Varela-Ortega *et al.* (2016) to simulate water irrigation requirement under climate change in the Guardiana basin in Spain and by Agarwal *et al.* (2019) to assess water demand for the Ur River watershed in India.

Climate change impact on the Nebhana dam system

Generation of climate change scenarios using LARS-WG

Daily weather data were generated using the Long Ashton Research Station Weather Generator (LARS-WG 6.0). This weather generator uses stochastic models to generate daily series of maximum and minimum temperatures, rainfall and solar radiation based on available daily climatic data for the period 1985–2004 to determine a set of parameters for probability distributions and correlations of the climatic data (Semenov *et al.* 1998). LARS-WG was also used to generate downscaled daily climatic data based on five GCMs of the CMIP5 under two RCPs, 4.5 and 8.5. LARS-WG 6.0 applies a statistical downscaled method called the Delta method or change factor method as an effective method to bridge the gaps between mismatched scales of GCM outputs

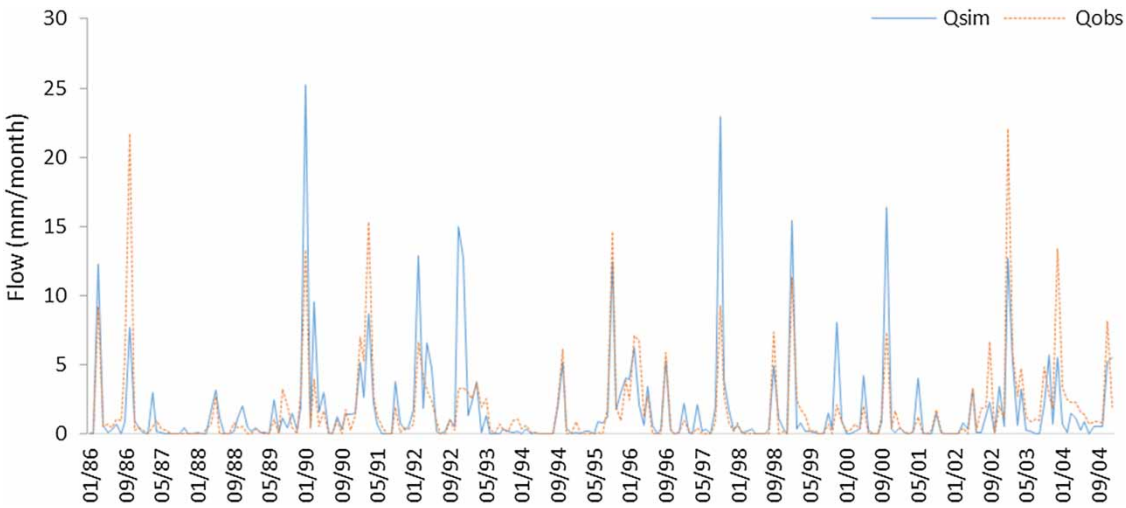

Figure 5 | Monthly observed and simulated discharge to the Nebhana dam over the calibration and validation periods.

and the scale of interest for regional impacts (Rahmati *et al.* 2019). LARS-WG has been largely used for generating long-term daily weather data as well as climate change scenarios based on different GCMs in Malaysia (Hassan *et al.* 2014), northern Syria and Lebanon (Dixit & Telleria 2015), Iran (Karamouz *et al.* 2013; Rouhani & Jafarzadeh 2017; Zamani *et al.* 2017) and Zambia (Chisanga *et al.* 2017).

The generated climatic data concern three periods of time, 2021–2040, 2041–2060 and 2061–2080 (Table 4).

Estimation of supply and demand under climate change scenarios using WEAP

WEAP software was used to evaluate the water supply and demand sustainability under climate change scenarios of the Nebhana dam system. The WEAP software was developed by the Stockholm Environment Institute (SEI) and is a decision support system software that is used to simulate and evaluate water management alternatives under different scenarios. WEAP can be used at municipal level, agricultural systems, basin systems or complex river systems. WEAP allows the reproduction of actual water management systems and permits the evaluation of different management practices. WEAP software has been largely used to answer water management issues in different areas. Faiz *et al.* (2018) used WEAP for hydrological model performance under GCM in China. Hussen *et al.* (2018) employed WEAP to analyse integrated water resources allocations under climate change scenarios. Hund *et al.* (2018) created a hydrological modelization to characterize the relationship between rainfall and groundwater recharge. Esteve *et al.* (2015) combined an economic optimization model with the hydrological model WEAP to represent socio-economic, agronomic and hydrological systems to cover the impact of climate change on the Guadiana basin in Spain. In Ghana, Okyereh *et al.* (2019) used WEAP to explore the consequences of climate change and variability on water resources availability, food security and environment in the Volta basin.

The Nebhana dam system model was constructed as shown in Figure 6.

Even though the WEAP hydrological model can simulate the inflow to the Nebhana dam, the GR2M model was applied to observe the impacts of temperature and precipitation changes on runoff under the generated future climates scenarios. Results were introduced directly as inputs to the model. The pipeline is represented in the WEAP model as transmission links from the Nebhana dam to each irrigated district (Figure 6). Finally, in this WEAP schematic, each irrigated district is represented by a catchment object as a water demand node. The model simulates the ETC as well as IWR for each represented crop in the irrigated districts using the MABIA approach.

To take into consideration the impact of climate change on ETc and IWR, the first step was to determine the length of the different crops' cycles for each generated climate according to their base temperature and heat requirement (GDD).

Also, other water demands can be represented as a demand site in WEAP without being estimated but rather introduced as input data. Water demands outside the Nebhana dam system were represented as a single demand site (Sahel (1) node in Figure 6) and monthly water demand was introduced based on averaged historical records obtained from the SECADENORD for the time period 2004–2017.

Since WEAP software allows multiple scenario analysis (Yates *et al.* 2015b), each generated climate scenario as well as each time period, including a baseline scenario, was run with its own specific input data regarding water inflow to the dam, climatic data and crops' characteristics (crop cycle and duration of each development stage). The results obtained were then averaged for each RCP emission scenario.

Table 4 | Generated climatic data under different models, RCP emissions scenarios for three periods of time

	Representative concentration pathways		Time period		
General circulation model	RCP 4.5	RCP 8.5	2021–2040	2041–2060	2061–2080
EC-EARTH	+	+	+	+	+
HadGEM2-ES	+	−	+	+	+
MIROC5	+	+	+	+	+
MPI-ESM-MR	+	+	+	+	+
GFDL-CM3	+	+	+	−	−

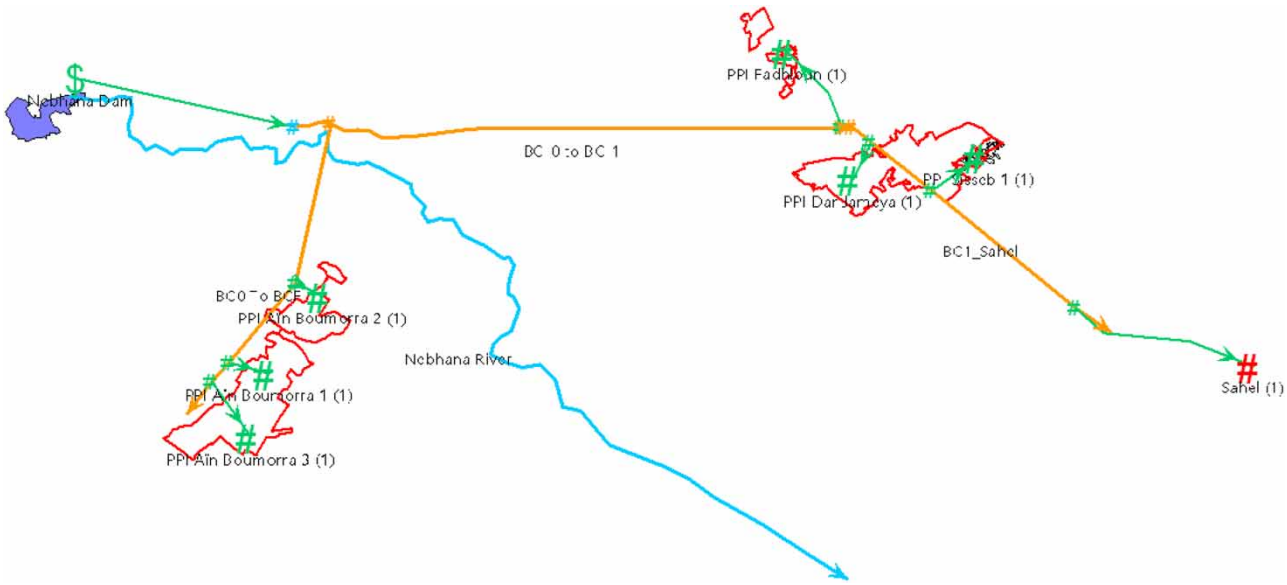

Figure 6 | Schematic representation of the Nebhana dam system in WEAP.

RESULTS

Reference evapotranspiration and rainfall changes

Table 5 shows the annual average and standard deviation of ETo and precipitation in the baseline (1985–2004) and under the two RCP emission scenarios RCP 4.5 and RCP 8.5 for the three periods, 2021–2040, 2041–2060 and 2061–2080. Concerning the baseline, the average ETo is 1,258 mm. For the first period (2021–2040), the ETo would increase to 1,317 mm under RCP 4.5 and 1,323 mm under RCP 8.5. During the second period (2041–2060), ETo would increase under RCP 4.5 and RCP 8.5 to attain 1,320 and 1,328 mm, respectively. Finally, for the third period (2061–2080), ETo is projected to increase to 1,341 mm under RCP 4.5 and 1,375 mm under RCP 8.5.

Regarding rainfall, during the historical period, the annual average rainfall is 300 mm with a high value of standard deviation of 75 mm. Under RCP 4.5 and RCP 8.5 emission scenarios, rainfall is expected to decrease for the three periods of time from 262 mm to 274 mm for RCP 4.5 and from 248 mm to 301 mm for RCP 8.5. Overall, in the future, an increase of ETo is expected to reach 6% on average, where rainfall could be reduced up to 8% under RCP 4.5 and RCP 8.5 emission scenarios. These changes could negatively impact not only the water supply but also the water demand of the Nebhana system.

Effect of climate change on the dam inflow

Climate change scenarios present a significant decrease in the annual inflow volume to the dam for the three periods of time 2021–2040, 2041–2060 and 2061–2080 and under the RCP 4.5 and RCP 8.5 emission scenarios (Figure 7).

Under the RCP 4.5 emission scenario, annual inflow is reduced by 28% in the first period, 14% in the second and

Table 5 | Average and standard deviation (in parentheses) of reference evapotranspiration and precipitation

	Reference evapotranspiration (mm)			Rainfall (mm)		
Period	**Baseline**	**RCP4.5**	**RCP8.5**	**Baseline**	**RCP4.5**	**RCP8.5**
2021–2040	1,258 (10)	1,317 (5)	1,323 (6)	300 (76)	274 (30)	286 (39)
2041–2060		1,320 (25)	1,328 (32)		261 (32)	301 (136)
2061–2080		1,341 (29)	1,375 (30)		262 (32)	248 (26)

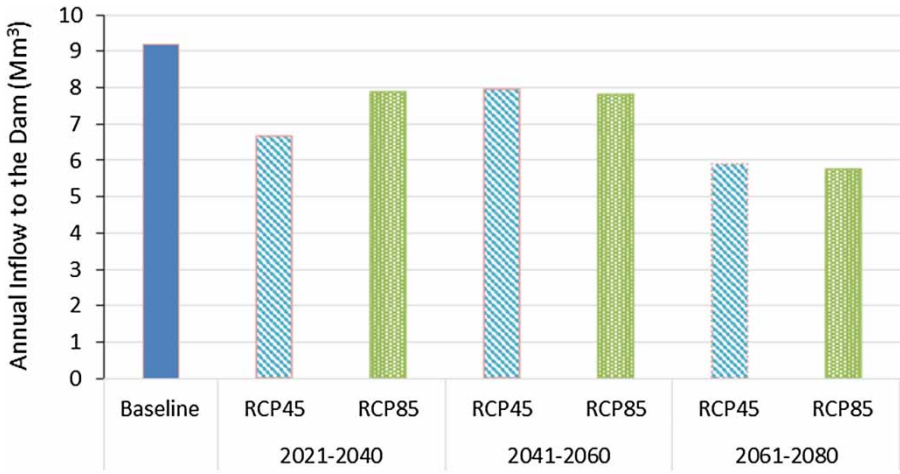

Figure 7 | Annual inflow to the reservoir under RCP emission scenarios.

36% in the third period. Under the RCP 8.5 scenario emission, a reduction of around 23%, 15% and 37% is noticed for the three periods of time. Concerning RCP 4.5, results show a decrease in annual flow during the first time period, then a relative increase during the second period, going from 6.65 Mm^3/year to 7.95 Mm^3/year. It also shows a decrease during the third period, reaching 5.88 Mm^3/year. This fluctuation was also reported by Milano *et al.* (2013) in the case of the Ebro basin, Spain, Ouyang *et al.* (2015) for the Huangnizhuang catchment in China and Reshmidevi *et al.* (2018) at the Malaprabha watershed in Bangladesh. The authors explain this sensitivity of runoff by the combination of increasing ETo and decreasing precipitation.

Monthly inflow to the dam shows similar changes to the annual inflow (Figure 8).

From the baseline data, it is important to notice that the winter season represents the period of the year with the highest inflow to the dam (40%) followed by autumn (30%), spring (25%) and summer (5%).

For the first period, 2021–2040, the reduction in monthly inflow is projected to range from 20% during summer to 40% during autumn under the RCP 4.5 emission scenario. In contrast, a slight increase of 3% is expected during spring. Under RCP 8.5, inflow is projected to decrease by 19% during autumn, 17% during winter, 1% during spring and 44% during summer (Figure 8(a)).

During the second period, 2041–2060, the decrease varies from 2% during winter to 48% during summer under RCP 4.5 and from 10% during spring to 35% during summer under RCP 8.5 (Figure 8(b)).

For the third period, 2061–2080, the decrease is substantially identical under the RCP 4.5 and 8.5 scenarios with 41% in autumn and 39% in winter. During spring, the decrease reaches 16% under RCP 4.5 and 24% under RCP 8.5 (Figure 8(c)).

Lespinas *et al.* (2014) report similar results on small Mediterranean coastal rivers where climate change scenarios led to a lower reduction during winter and a higher discharge reduction during summer than spring and autumn seasons.

Impact of climate change on crop cycle duration

According to their thermal characteristics (base temperature and GDD_{cycle}), crops' cycle length is expected to shorten during the three time periods and under both RCP emission scenarios (Table 6). The main affected crops are olive and citrus where the decrease would vary from 22.4 to 27.9% and from 28.9 to 34.6%, respectively. The least affected crops are wheat, oat and potato with an average reduction of 5.4, 6.3 and 6.4%, respectively.

The findings of this study agree with the results reported by Pathak & Stoddard (2018), who pointed out that the tomato growing season length in California would be reduced between 11 and 13% under RCP 4.5 and between 13 and 14% under RCP 8.5. Moreover, Saadi *et al.* (2015)

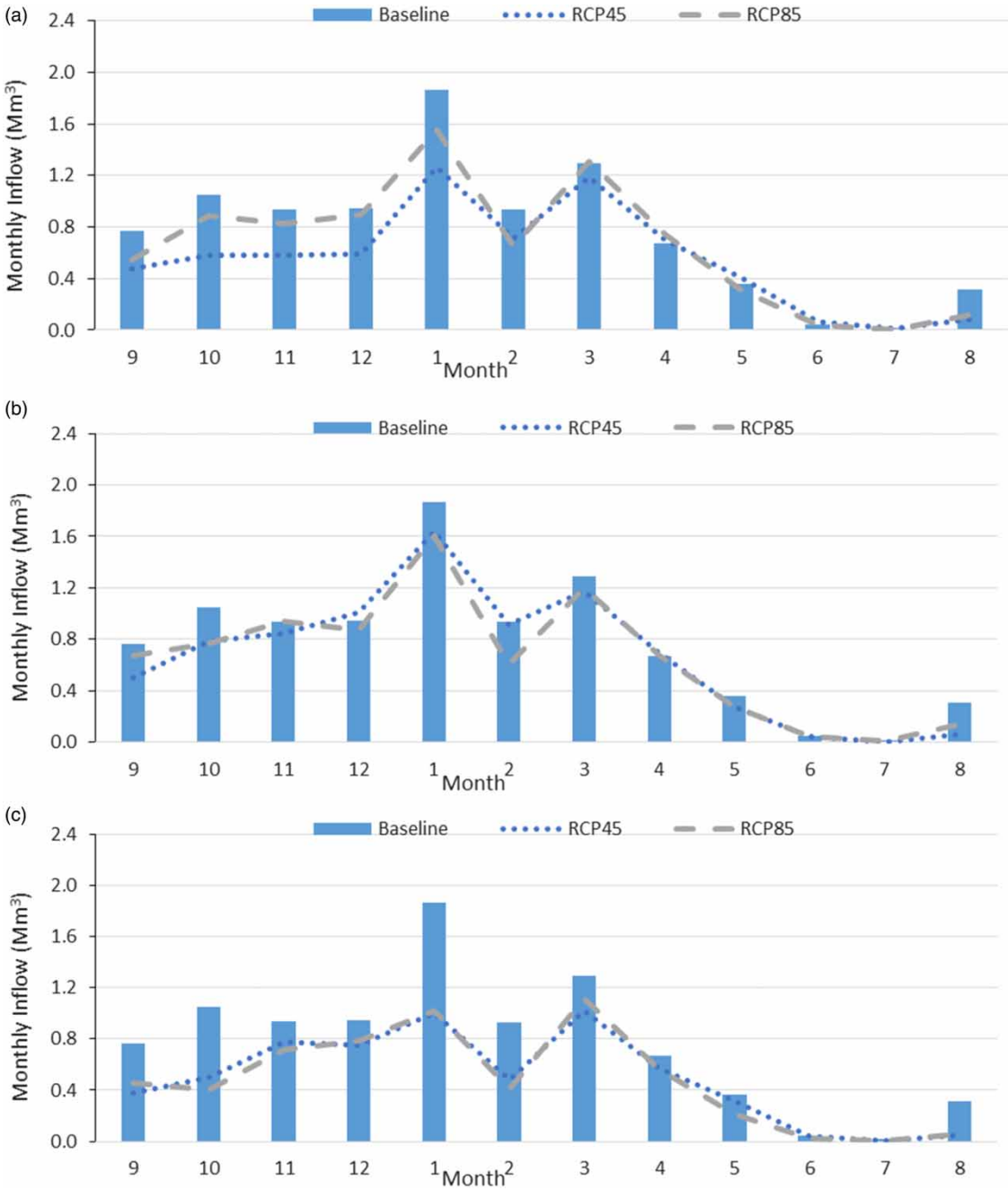

Figure 8 | Monthly inflow volume to the dam under RCP 4.5 and RCP 8.5 during (a) 2021–2040, (b) 2041–2060 and (c) 2061–2080 time periods.

indicate a 9.6% reduction in tomato length cycle under A1B emission scenarios in Mediterranean regions. Our result is also consistent with the findings of Chattaraj *et al.* (2014) and Saadi *et al.* (2015), where the projected higher temperatures shortened the wheat growing season by 5 to 15% in India and by 6.9 to 8% in Mediterranean regions.

Impact of climate change on crop water requirement

The ETo, ETc, rainfall and IWR for each crop averaged over the GCM projections under RCP 4.5 and RCP 8.5 emission scenarios in the first period, 2021–2040, are presented in Table 7. For the present, the seasonal ETc

Table 6 | Average length of the growing season for historical records and future climate projections (in days)

			Period/RCP					
			2021–2040		2041–2060		2061–2080	
Crop	Typical planting Date/Bud burst	Actual length cycle (days)	RCP 4.5	RCP 8.5	RCP 4.5	RCP 8.5	RCP 4.5	RCP 8.5
Olive tree	05/03	270	210	207	206	201	202	195
Citrus	05/02	360	256	253	253	247	245	235
Apricot	20/02	240	225	223	222	219	220	216
Pomegrenate	01/03	275	237	234	233	227	228	221
Almond tree	15/02	305	274	272	269	263	265	258
Pepper	20/04	215	187	185	184	179	181	175
Green peas AB	01/09	172	142	140	134	129	129	116
Green peas Sisseb	15/10	172	157	155	151	146	146	136
Faba bean	01/11	155	142	140	138	133	134	125
Potato	15/02	94	90	89	89	88	88	84
Onion	01/09	95	86	86	84	82	82	77
Tomato	10/03	90	84	83	83	81	81	77
Wheat	15/12	180	173	172	172	170	169	165
Barley	20/11	175	166	164	163	159	160	153
Oat	15/12	170	163	162	161	159	158	153
Cucumber	15/03	80	73	72	72	71	70	66

ranged from 257 mm for cucumber to 1,074 mm for citrus, with a standard deviation of 17 mm and 88 mm, respectively.

The results show that for the first period, 2021–2040, despite an increase in annual ETo, a decrease in ETc is expected for all crops. For the fruit trees, citrus and olive are expected to have the highest decrease under both emission scenarios reaching on average 12.9% and 11.8%, respectively. Regarding cereals, where the decrease in ETc for oat and wheat does not exceed 5% under the two RCP emission scenarios, the barley crop reaches a 7.9% decrease under RCP 8.5. Finally, for vegetables, summer crops such as pepper and tomato, the decrease in ETc remains relatively low compared to winter vegetables where the decrease in ETc reaches 15.3% for green peas and 18.2% for faba bean.

For the middle period (2041–2060), fruit trees' ETc would decrease from 2.1% for apricot to 17% for olive trees, under the RCP 4.5 and RCP 8.5 emission scenarios (Table 8). For cereals, barley crop would have the highest decrease reaching 10.3% under RCP 8.5. The same tendency is observed for winter vegetable crops where faba beans would have the highest reduction of ETc with 19.8% and 22.8% under RCP 4.5 and RCP 8.5, respectively. Similarly, a drop of summer vegetable ETc is projected reaching 8.8% for cucumber under both RCP emission scenarios and 7.2% for tomato under RCP 8.5.

Finally, for the last period (2061–2080), under the RCP 4.5 and RCP 8.5 scenarios, respectively, ETc could be lower by 9.2% and 9.5% for fruit trees, 7.4% and 10.5% for cereals, 19.6% and 22.5% for winter vegetables and 8.3% and 12.1% for summer vegetables (Table 9).

Overall, the pattern of ETc followed the pattern of crop season length changes under the two RCP emission scenarios. Recent studies also suggest that increased temperatures and changes in crops' cycle patterns can significantly decrease the ETc. Shortening crops' cycle may be the main reason for the decrease in ETc. The ETc is expected to decrease in many countries due to climate change. Acharjee *et al.* (2017) reported that boro rice ETc could decrease by 17.6% in Bangladesh. Saadi *et al.* (2015) reported the same tendency for winter wheat and tomato

Table 7 | Temporal change in reference evapotranspiration, crop evapotranspiration, rainfall and irrigation water requirement (in mm) during crop cycles for the period 2021–2040 with standard deviation given in parentheses

	Baseline				RCP 4.5				RCP 8.5			
Crop	ETo	ETc	Rain	IWR	ETo	ETc	Rain	IWR	ETo	ETc	Rain	IWR
Apricot tree	1,049 (39)	929 (48)	168 (67)	769 (50)	1,056 (33)	918 (7)	145 (58)	794 (47)	1,053 (31)	910 (3)	150 (60)	785 (39)
Citrus	1,229 (82)	1,074 (88)	288 (99)	812 (93)	1,137 (50)	937 (9)	178 (67)	766 (72)	1,133 (49)	934 (6)	188 (73)	757 (72)
Almond	1,159 (62)	1,021 (72)	242 (84)	841 (77)	1,172 (58)	1,015 (5)	200 (76)	765 (44)	1,169 (57)	1,010 (4)	206 (80)	782 (51)
Oat	469 (8)	444 (16)	147 (38)	263 (38)	451 (8)	424 (5)	131 (49)	269 (45)	448 (7)	426 (5)	141 (49)	258 (55)
Wheat	522 (8)	506 (14)	149 (39)	318 (52)	508 (9)	490 (5)	137 (50)	321 (54)	503 (7)	495 (4)	149 (49)	312 (58)
Cucnmber	283 (6)	257 (17)	78 (35)	131 (26)	261 (6)	237 (1)	65 (32)	151 (33)	259 (6)	239 (1)	73 (42)	143 (29)
Faba bean	302 (5)	303 (13)	136 (50)	161 (37)	255 (5)	248 (3)	120 (46)	134 (27)	252 (5)	248 (3)	120 (53)	139 (31)
Pomegranate	1,111 (57)	910 (64)	215 (86)	712 (73)	1,090 (40)	876 (9)	161 (63)	739 (45)	1,087 (38)	867 (3)	168 (66)	731 (58)
Onion	266 (6)	209 (32)	115 (77)	199 (22)	265 (6)	203 (2)	106 (51)	192 (27)	265 (6)	197 (2)	105 (56)	187 (30)
Olive tree	1,100 (56)	629 (53)	213 (86)	403 (39)	1,016 (31)	560 (11)	137 (54)	406 (79)	1,011 (28)	550 (4)	138 (59)	388 (66)
Barley	405 (6)	392 (20)	159 (49)	219 (52)	378 (7)	364 (4)	138 (45)	212 (45)	375 (6)	362 (4)	145 (51)	206 (55)
Potato	312 (6)	300 (19)	85 (34)	186 (21)	305 (7)	293 (4)	77 (37)	214 (24)	304 (6)	296 (3)	83 (43)	207 (19)
Green peas Ain Boumorra	376 (5)	320 (32)	183 (82)	213 (31)	340 (6)	279 (3)	155 (61)	207 (35)	338 (7)	272 (3)	154 (65)	207 (36)
Green peas Sisseb	326 (5)	330 (16)	162 (63)	190 (38)	292 (6)	281 (3)	132 (49)	163 (33)	289 (6)	279 (1)	137 (57)	159 (34)
Pepper	948 (54)	802 (98)	162 (84)	818 (58)	939 (45)	800 (16)	120 (51)	835 (46)	936 (44)	797 (10)	124 (52)	832 (47)
Tomato	358 (8)	344 (19)	84 (38)	239 (31)	339 (7)	321 (0)	74 (35)	233 (39)	339 (6)	328 (2)	83 (45)	228 (33)

Table 8 | Temporal change in reference evapotranspiration, crop evapotranspiration, rainfall and irrigation water requirement (in mm) during crop cycles for the period 2041–2060 with standard deviation given in parentheses

	Baseline				RCP 4.5				RCP 8.5			
Crop	ETo	ETc	Rain	IWR	ETo	ETc	Rain	IWR	ETo	ETc	Rain	IWR
Apricot tree	1,049 (39)	929 (48)	168 (67)	769 (50)	1,052 (38)	936 (40)	124 (51)	792 (46)	1,049 (35)	939 (34)	133 (51)	787 (66)
Citrus	1,229 (82)	1,074 (88)	288 (99)	812 (93)	1,140 (33)	963 (37)	166 (64)	787 (60)	1,136 (28)	958 (32)	162 (65)	777 (77)
Almond	1,159 (62)	1,021 (72)	242 (84)	841 (77)	1,177 (35)	1,035 (48)	179 (68)	844 (56)	1,177 (29)	1,035 (38)	177 (70)	843 (76)
Oat	469 (8)	444 (16)	147 (38)	263 (38)	444 (9)	427 (13)	131 (50)	263 (52)	435 (8)	418 (15)	124 (52)	260 (61)
Wheat	522 (8)	506 (14)	149 (39)	318 (52)	498 (9)	496 (11)	136 (50)	324 (51)	490 (9)	485 (13)	128 (54)	320 (54)
Cucumber	283 (6)	257 (17)	78 (35)	131 (26)	283 (6)	263 (13)	60 (25)	137 (27)	283 (6)	263 (13)	60 (25)	137 (27)
Faba bean	302 (5)	303 (13)	136 (50)	161 (37)	245 (6)	248 (12)	115 (53)	141 (30)	235 (6)	239 (11)	117 (51)	138 (42)
Pomegranate	1,111 (57)	910 (64)	215 (86)	712 (73)	1,097 (31)	909 (41)	148 (60)	744 (59)	1,092 (26)	902 (35)	147 (57)	734 (61)
Onion	266 (6)	209 (32)	115 (77)	199 (22)	260 (25)	245 (29)	95 (59)	186 (32)	261 (21)	246 (21)	101 (51)	181 (42)
Olive tree	1,100 (56)	629 (53)	213 (86)	403 (39)	1,019 (25)	551 (35)	116 (47)	402 (74)	1,008 (20)	546 (30)	117 (42)	393 (93)
Barley	405 (6)	392 (20)	159 (49)	219 (52)	367 (7)	365 (13)	138 (53)	207 (49)	357 (7)	358 (13)	132 (53)	203 (57)
Potato	312 (6)	300 (19)	85 (34)	186 (21)	302 (7)	304 (9)	69 (35)	213 (22)	298 (6)	301 (8)	68 (42)	216 (28)
Green peas Ain Boumorra	376 (5)	320 (32)	183 (82)	213 (31)	330 (26)	312 (30)	142 (69)	213 (34)	329 (22)	313 (22)	146 (62)	204 (45)
Green peas Sisseb	326 (5)	330 (16)	162 (63)	190 (38)	299 (8)	290 (15)	141 (56)	164 (33)	299 (8)	284 (14)	143 (55)	169 (43)
Pepper	948 (54)	802 (98)	162 (84)	818 (58)	944 (30)	963 (39)	108 (51)	848 (46)	940 (24)	961 (33)	109 (46)	848 (46)
Tomato	358 (8)	344 (19)	84 (38)	239 (31)	341 (8)	335 (10)	67 (32)	241 (37)	333 (7)	326 (12)	64 (37)	239 (62)

Table 9 | Temporal change in reference evapotranspiration, crop evapotranspiration, rainfall and irrigation water requirement (in mm) during crop cycles for the period 2061–2080 with standard deviation given in parentheses

	Baseline				RCP 4.5				RCP 8.5			
Crop	ETo	ETc	Rain	IWR	ETo	ETc	Rain	IWR	ETo	ETc	Rain	IWR
Apricot tree	1,049 (39)	929 (48)	168 (67)	769 (50)	899 (41)	899 (41)	125 (43)	791 (50)	902 (41)	902 (41)	111 (43)	810 (49)
Citrus	1,229 (82)	1,074 (88)	288 (99)	812 (93)	1,140 (37)	925 (33)	158 (61)	780 (68)	1,143 (41)	922 (32)	139 (51)	797 (64)
Almond	1,159 (62)	1,021 (72)	242 (84)	841 (77)	1,184 (38)	1,004 (47)	173 (61)	844 (62)	1,197 (43)	1,012 (47)	154 (56)	884 (61)
Oat	469 (8)	444 (16)	147 (38)	263 (38)	437 (8)	413 (18)	128 (45)	266 (54)	418 (9)	401 (16)	119 (49)	266 (52)
Wheat	522 (8)	506 (14)	149 (39)	318 (52)	496 (9)	485 (19)	136 (48)	323 (52)	481 (10)	477 (16)	126 (50)	333 (51)
Cucumber	283 (6)	257 (17)	78 (35)	131 (26)	254 (6)	229 (18)	64 (35)	148 (29)	245 (7)	211 (15)	54 (33)	154 (27)
Faba bean	302 (5)	303 (13)	136 (50)	161 (37)	236 (6)	236 (13)	119 (56)	142 (34)	231 (8)	218 (14)	106 (40)	141 (29)
Pomegranate	1,111 (57)	910 (64)	215 (86)	712 (73)	1,098 (35)	879 (47)	139 (51)	754 (60)	1,099 (38)	872 (46)	121 (48)	767 (60)
Onion	266 (6)	209 (32)	115 (77)	199 (22)	262 (29)	189 (30)	89 (54)	193 (34)	261 (29)	191 (28)	78 (38)	197 (37)
Olive tree	1,100 (56)	629 (53)	213 (86)	403 (39)	1,010 (26)	532 (33)	111 (39)	395 (65)	1,005 (28)	521 (30)	100 (40)	403 (65)
Barley	405 (6)	392 (20)	159 (49)	219 (52)	360 (7)	355 (14)	129 (54)	211 (53)	340 (9)	335 (17)	119 (51)	212 (50)
Potato	312 (6)	300 (19)	85 (34)	186 (21)	298 (7)	280 (17)	71 (37)	220 (22)	289 (7)	270 (16)	63 (36)	222 (23)
Green peas Ain Boumorra	376 (5)	320 (32)	183 (82)	213 (31)	329 (30)	262 (28)	131 (69)	215 (42)	324 (32)	265 (28)	117 (41)	223 (40)
Green peas Sisseb	326 (5)	330 (16)	162 (63)	190 (38)	270 (9)	265 (16)	137 (61)	168 (34)	249 (11)	241 (16)	119 (39)	161 (35)
Pepper	948 (54)	802 (98)	162 (84)	818 (58)	944 (33)	799 (59)	101 (49)	866 (50)	952 (36)	802 (63)	91 (35)	891 (55)
Tomato	358 (8)	344 (19)	84 (38)	239 (31)	332 (8)	316 (19)	70 (34)	236 (36)	318 (8)	297 (19)	63 (33)	240 (35)

in the Mediterranean countries and Chen *et al.* (2010) regarding wheat and maize in the North China Plain.

Impact of climate change on irrigation water requirement

IWR results turned out to be diverse depending on crops, as well as RCP emission scenarios and the time period.

During the first time period, 2021–2040, despite the decrease of ETc under RCP 4.5, IWR results are variable (Table 7). Fruit trees, citrus and almond will register a decrease in irrigation demand (7.3%) whereas olive, apricot and pomegranate will show an increase (2.3%) reaching 3.8% for pomegranate. As for cereals, only barley will have a decrease in IWR of 3% while for wheat and oat, IWR would increase by 0.8% and 2.4%, respectively. For fava bean and green peas, an important decrease in irrigation demand is expected, attaining 17%, whereas potato and cucumber show an increase of 15%. Under RCP 8.5, the majority of crops will undergo a decrease in IWR varying from 2% for oat and wheat to 16.3% for green peas. The increase concerns only apricot, pomegranate, pepper, cucumber and potato with 2.1%, 2.7%, 1.7%, 9.4% and 11.5%, respectively.

For the second time period (2041–2060), the IWR variation is low under the two RCP emission scenarios (Table 8). Whether it is an increase or a decrease, results show that the variation never exceeds 5% except for some crops. Cucumber and potato IWRs would face an increase of 12.9% and 11.1% under both RCPs whereas green peas and fava bean IWRs would decrease, reaching 10.1% and 15.7% respectively, under RCP 8.5. For fruit trees, the highest increase is observed in pomegranate with 5.7% and 4.2% under RCP 4.5 and RCP 8.5, respectively. The highest decrease is observed with citrus with 6% under RCP 8.5 and 4.7% under RCP 4.5, respectively. For cereals, a decrease in IWR attains 7.4% under RCP 8.5.

Similarly, during the third time period, 2061–2080, results indicate a slow variation in IWR for the majority of crops under RCP 4.5 and RCP 8.5 (Table 9). Under RCP 4.5, half of the crops show an average increase of 3.9% in irrigation demand with a maximum of 14.1% for potato. The decrease in IWR is about 4.8% on average with a highest value of 14% for fava bean. For fruit trees, variation in irrigation requirement reaches a maximum decrease of 6.2% for citrus and the highest increase of 4.3% for pomegranate. As for cereals, only wheat shows a small increase of 1.4% in IWR. Under RCP 8.5, IWR would increase for the majority of crops with a maximum of 6% for pomegranate regarding fruit trees, 4.5% for wheat concerning cereals and 15.4% for potato.

These results support previous findings in the literature, such as those of Hong *et al.* (2016) for barley and wheat crops in South Korea under RCP 4.5 and RCP 8.5, Fares *et al.* (2017) for major producing areas of citrus in the world under RCP 4.5 and Zhou *et al.* (2017) for wheat in China where because of the rain pattern change, IWR would not necessarily be affected at a high rate under different climate scenarios.

Estimation of supply and demand of the Nebhana dam system under climate change scenarios

Table 10 summarizes the annual irrigation demand of the Nebhana dam system during the three time periods and under the two RCP emission scenarios. Results show that

Table 10 | Annual irrigation demand of the study area (in Mm^3) and water demand coverage (in %) of the Nebhana dam under climate change scenarios with and without water transfer

	Annual irrigation demand (in Mm^3)			Water demand coverage by the Nebhana dam under climate change scenarios (in %)			
				With water transfer outside		Absence of water transfer	
Period	Baseline	RCP 4.5	RCP 8.5	RCP 4.5	RCP 8.5	RCP 4.5	RCP 8.5
2021–2040	9.79	9.86	9.72	29%	34%	68%	81%
2041–2060	9.89	9.96	10.12	34%	33%	79%	77%
2061–2080	9.88	9.94	10.21	25%	24%	59%	56%

the system irrigation demand does not vary significantly under the two RCPs compared to the baseline. Under RCP 4.5, the potential change in irrigation demand does not exceed 1% and a maximum increase of 3.6% would occur during the third period, 2061–2080, under RCP 8.5. Similar results were found by Wang *et al.* (2016) in the Baojixia Irrigation District in China where irrigation water demand would not differ much between different climatic scenarios and will not increase at the same rate as the temperature rise. This low variability is explained by the fact that 55% of the irrigated area is cropped by olive and apricot trees. As shown in the previous section, IWR of these two crops will not be highly impacted under climate change, with a decrease below 7% compared to the baseline.

As these results show, irrigation demand would not be greatly impacted under climate change scenarios. However, as shown in the previous section, the inflow to the reservoir would decrease significantly.

When analysing demand and supply of the Nebhana dam system for the period 2007–2017, results show that the Nebhana dam system does not meet its own water requirement. In fact, during this period, cumulated water volume in the reservoir only covered 89% of the actual water demand. This level of coverage was only attained because the Nebhana reservoir was filled, for the third time since its construction, at full capacity during the growing season which lasted between 2011 and 2012. Under the climate change scenario, the gap between supply and demand would be exacerbated as shown in Table 10.

Therefore, the situation is expected to degrade under RCP 4.5 and RCP 8.5, where the Nebhana dam system would undergo a stress situation covering only 25% of the water demand for the period of 2061–2080. Rochdane *et al.* (2012) suggested the same trend in the Rheraya watershed in Morocco, where the unmet demand of the system could reach 70% under B2 scenario when no adaptation strategies are proposed.

The irrigation requirement's calculation for the study area was programmed as optimal irrigation, and the water demand outside the study area was considered as an averaged constant and represents roughly 13 $Mm^3\,year^{-1}$. If this water transfer outside the study area is removed as an adaptation scenario, the supply from the Nebhana dam could cover a significant part of the irrigation demand, as shown in Table 10.

In fact, under RCP 4.5, during the period 2021–2040, supply from the Nebhana dam could ensure 68% of the irrigation demand, 79% for the period 2041–2060 and drop to 59% for the period 2061–2080. Under the RCP 8.5 emission scenario, supply could cover 81% of the irrigation demand during the period 2021–2040 and drop to 56% during the period 2061–2080.

DISCUSSION AND CONCLUSION

This study examined the impacts of climate change on the irrigation supply and demand of the Nebhana dam system. Stochastically downscaled GCM models based on CMIP5 scenarios were combined with two RCP emission scenarios (RCP 4.5 and RCP 8.5), using LARS-WG for the three time periods, 2021–2040, 2041–2060 and 2061–2080. Based on the GR2M hydrological model, water inflow to the Nebhana reservoir was calibrated and validated and then simulated under climate change scenarios. Built on climate change generated data, expected crop cycle lengths were estimated using the GDD for each crop and each GCM for the three periods of time. Finally, a WEAP model of the Nebhana dam system was constructed including the reservoir, the irrigated districts and the demand site of the Sahel outside the system.

Results show an increase in ETo under the two RCPs during the three time periods varying from 4.9 to 10%, and a decrease in annual rainfall under RCP 4.5 and RCP 8.5 reaching up to 17.5%. Lhomme *et al.* (2009) found for the same area a similar increase in ETo but also an increase in precipitation, which the authors explained by the difficulty in predicting the rainfall events. Increased ETo could potentially exceed precipitation, resulting in more intense droughts and therefore a reduction in water inflow and an increase in irrigation in the Nebhana dam system.

Annual inflow to the Nebhana reservoir is expected to decrease up to 37% for both the RCP 4.5 and RCP 8.5 emission scenarios. In the Chiba watershed, a small Mediterranean catchment located approximately 100 km north-east of the study area in Tunisia, annual runoff is likely to fall between 25% and 48% compared to the

baseline (Sellami *et al.* 2016). Despite having only two free parameters, the GR2M has been shown to perform well when compared to similar models (Mouelhi *et al.* 2006) and provided a good quality of the hydrological simulations in terms of NSE criteria for the study area. However, the GR2M model failed to reproduce the intensity of high inflows and tended to underestimate it, which can alter the availability of water, and this should be further improved.

This study also provided a quantitative approach to estimate and quantify the crop water requirements as well as the irrigation water requirements for the main crops of the area under climate change. Using MABIA, the ETc and IWR of 16 crops were estimated under climate change. A database of crop, soil and meteorological data was constructed and then a study using climate predictions for the future (2021–2080) using the RCP 4.5 and RCP 8.5 climate change scenarios was conducted.

Concerning crop water requirement, due to the reduction of the growth cycle, a decrease in ETc is expected to occur under both RCP emission scenarios and for the three periods of time. The most affected crops were winter vegetables, mainly fava bean and green peas, as well as olive with a decrease of 16.9% under RCP 4.5 and 18.9% under RCP 8.5. These decreases in ETc are mainly explained by the reduction of the crop growth cycle despite the annual increase of ETo. Studies of single crops found the same tendency regarding the decrease of ETc, such as Chowdhury *et al.* (2016) for wheat, barley, tomato, potato and citrus in Saudi Arabia, Fares *et al.* (2017) for citrus in Tunisia. However, high temperatures should be analysed as they may become a limiting factor for plant productivity and decrease crop yields. Also, as studied by Zeroual *et al.* (2019), climate change would potentially bring a shift in the bioclimatic stage and cause numerous problems related to food safety and plant adaptation.

Concerning IWR, the results are more nuanced depending on the crops, the RCP emission scenarios and the time period. For the main crops in terms of land use, namely, olive, apricot, citrus and green peas, irrigation requirement variability remains relatively low and except for apricot, shows a decrease under both RCP emission scenarios. This is mainly explained by the rainfall variation and the growth period of crops. In the study, IWR was estimated based on an optimal irrigation scheduling and further research should take into account actual practices where applied water for each crop is governed by economic constraints.

Finally, in regards to the global water balance of the system, it appears that the water resources currently do not meet the demand system requirement. The situation could get worse under climate change, unless the water demand outside the study area is supplied from another source.

The integrated modelling approach presented here provides a meaningful framework to analyse the status of a small Mediterranean basin under changing climate conditions. It also can be a basis for identifying adaptation measures and simulating their potential impacts. Future directions for this research include the investigation of other adaptation measures scenarios. Such scenarios could permit more flexible water allocation such as prioritizing water allocation diversion to permanent crops during drought periods, improving deficit irrigation strategies or diversifying land use. Such studies require a participative approach from water users, water managers and scientists.

ACKNOWLEDGEMENT

The authors wish to thank the CREM-BGR Project for providing financial support for the data collection. They also thank Dr Hans-Werner Müller of the Federal Institute for Geosciences and Natural Resources (BGR) for his support during this work. Thanks are also due to Dr Mohamed Jabloun for his assistance, advice and comments.

REFERENCES

Abdal, M. & Suleiman, M. 2004 Irrigation Water Management for Agricultural Development in Kuwait. In: *Irrigation Water Management for Agricultural Development in Uttar Pradesh, India*. Springer International Publishing, pp. 1–5. https://doi.org/10.1061/40430(1999)148.

Abeysingha, N. S., Islam, A. & Singh, M. 2018 Assessment of climate change impact on flow regimes over the Gomti River basin under IPCC AR5 climate change scenarios. *Journal of Water and Climate Change* jwc2018039. https://doi.org/10.2166/wcc.2018.039.

Acharjee, T. K., Ludwig, F., van Halsema, G., Hellegers, P. & Supit, I. 2017 Future changes in water requirements of Boro rice in the face of climate change in North-West Bangladesh. *Agricultural Water Management* **194**, 172–183. https://doi.org/10.1016/j.agwat.2017.09.008.

Adgolign, T. B., Rao, G. V. R. S. & Abbulu, Y. 2016 WEAP modeling of surface water resources allocation in Didessa Sub-Basin. *West Ethiopia. Sustainable Water Resources Management* **2** (1), 55–70. https://doi.org/10.1007/s40899-015-0041-4.

Agarwal, S., Patil, J. P., Goyal, V. C. & Singh, A. 2019 Assessment of water supply–demand using water evaluation and planning (WEAP) model for Ur River watershed, Madhya Pradesh, India. *Journal of The Institution of Engineers (India): Series A* **100** (1), 21–32. https://doi.org/10.1007/s40030-018-0329-0.

Ahmad, S., Abbas, G., Ahmed, M., Fatima, Z., Anjum, M. A., Rasul, G., Khan, M. A. & Hoogenboom, G. 2019 Climate warming and management impact on the change of phenology of the rice-wheat cropping system in Punjab, Pakistan. *Field Crops Research* **230**, 46–61. https://doi.org/10.1016/j.fcr.2018.10.008.

Ahmed, K. F., Wang, G., Silander, J., Wilson, A. M., Allen, J. M., Horton, R. & Anyah, R. 2013 Statistical downscaling and bias correction of climate model outputs for climate change impact assessment in the U.S. northeast. *Global and Planetary Change* **100**, 320–332. https://doi.org/10.1016/j.gloplacha.2012.11.003.

Ahn, K. H. & Merwade, V. 2014 Quantifying the relative impact of climate and human activities on streamflow. *Journal of Hydrology* **515**, 257–266. https://doi.org/10.1016/j.jhydrol.2014.04.062.

Alkama, R., Marchand, L., Ribes, A. & Decharme, B. 2013 Detection of global runoff changes: results from observations and CMIP5 experiments. *Hydrology and Earth System Sciences* **17**, 2967–2979. https://doi.org/10.5194/hess-17-2967-2013.

Allani, M., Mezzi, R., Abdallah, W., Gharbi, A., Zouabi, A., Hedhli, K., Beji, R., Jemli, A., Mansouri Joumade, F., Afli, A., Hamza, M. E., Müller, H. W. & Sahli, A. 2018 A contribution to an advisory plan for integrated irrigation water management at Nebhana dam system: from research to operational support. *EPiC Series in Engineering* **3**, 26–15. https://doi.org/10.29007/vgpn.

Allen, R. G., Luis, S. P., Raes, D. & Smith, M. 1998 *Crop Evapotranspiration (Guidelines for Computing Crop Water Requirements)*. FAO Irrigation and Drainage Paper No. 56. FAO, Rome, Italy. https://doi.org/10.1016/j.eja.2010.12.001.

Al-Safi, H. I. J. & Sarukkalige, P. R. 2017 Evaluation of the impacts of future hydrological changes on the sustainable water resources management of the Richmond River catchment. *Journal of Water and Climate Change* **9** (1), 137–155. https://doi.org/10.2166/wcc.2017.144.

Al-Safi, H. I. J., Kazemi, H. & Sarukkalige, P. R. 2020 Comparative study of conceptual versus distributed hydrologic modelling to evaluate the impact of climate change on future runoff in unregulated catchments. *Journal of Water and Climate Change* **11** (2), 341–366. https://doi.org/10.2166/wcc.2019.180.

Bachir, S., Nouar, B., Hicham, C., Azzedine, H. & Larbi, D. 2015 Application of GR2M for rainfall-runoff modeling in Kébir Rhumel Watershed, north east of Algeria. *World Applied Sciences Journal* **33** (10), 1623–1630. https://doi.org/10.5829/idosi.wasj.2015.33.10.367.

Bai, P., Liu, X., Liang, K. & Liu, C. 2015 Comparison of performance of twelve monthly water balance models in different climatic catchments of China. *Journal of Hydrology* **529**, 1030–1040. https://doi.org/10.1016/j.jhydrol.2015.09.015.

Blöschl, G. & Montanari, A. 2010 Climate change impacts – throwing the dice? *Hydrological Processes* **24**, 374–381. https://doi.org/10.1002/hyp.7574.

Bottcher, A. B., Whiteley, B. J., James, A. I. & Hiscock, J. G. 2012 Watershed assessment model (WAM): model use, calibration, and validation. *Transactions of the ASABE* **55** (4), 1367–1383.

Cannon, A. J., Sobie, S. R. & Murdock, T. Q. 2015 Bias correction of GCM precipitation by quantile mapping: How well do methods preserve changes in quantiles and extremes? *Journal of Climate* **28** (17), 6938–6959. https://doi.org/10.1175/JCLI-D-14-00754.1.

Chattaraj, S., Chakraborty, D., Sehgal, V. K., Paul, R. K., Singh, S. D., Daripa, A. & Pathak, H. 2014 Predicting the impact of climate change on water requirement of wheat in the semi-arid Indo-Gangetic Plains of India. *Agriculture, Ecosystems and Environment* **197**, 174–183. https://doi.org/10.1016/j.agee.2014.07.023.

Chen, C., Wang, E., Yu, Q. & Zhang, Y. 2010 Quantifying the effects of climate trends in the past 43 years (1961–2003) on crop growth and water demand in the North China Plain. *Climatic Change* **100** (3), 559–578. https://doi.org/10.1007/s10584-009-9690-3.

Chen, H., Guo, J., Zhang, Z. & Xu, C. Y. 2013 Prediction of temperature and precipitation in Sudan and South Sudan by using LARS-WG in future. *Theoretical and Applied Climatology* **113** (3–4), 363–375. https://doi.org/10.1007/s00704-012-0793-9.

Chisanga, C. B., Phiri, E. & Chinene, V. R. N. 2017 Statistical downscaling of precipitation and temperature using long ashton research station weather generator in Zambia: a case of mount makulu agriculture research station. *American Journal of Climate Change* **6** (3), 487–512. https://doi.org/10.4236/ajcc.2017.63025.

Chowdhury, S., Al-Zahrani, M. & Abbas, A. 2016 Implications of climate change on crop water requirements in arid region: an example of Al-Jouf, Saudi Arabia. *Journal of King Saud University – Engineering Sciences* **28** (1), 21–31. https://doi.org/10.1016/j.jksues.2013.11.001.

Coron, L., Thirel, G., Delaigue, O., Perrin, C. & Andréassian, V. 2017 The suite of lumped GR hydrological models in an R package. *Environmental Modelling and Software* **94**, 166–171. https://doi.org/10.1016/j.envsoft.2017.05.002.

Cramer, W., Guiot, J., Fader, M., Garrabou, J., Gattuso, J. P., Iglesias, A., Lange, M. A., Lionello, P., Llasat, M. C., Paz, S., Peñuelas, J., Snoussi, M., Toreti, A., Tsimplis, M. N. & Xoplaki, E. 2018 Climate change and interconnected risks to sustainable development in the Mediterranean. *Nature Climate Change* **8**, 972–980. https://doi.org/10.1038/s41558-018-0299-2.

Daggupati, P., Pai, N., Ale, S., Zeckoski, R. W., Jeong, J., Parajuli, P. B., Saraswat, D. & Youssef, M. A. 2015 A recommended calibration and validation strategy for hydrologic and water quality models. *Transactions of the ASABE* **58** (6), 1705–1719. https://doi.org/10.13031/trans.58.10712.

Dixit, P. N. & Telleria, R. 2015 Advancing the climate data driven crop-modeling studies in the dry areas of Northern Syria and Lebanon: an important first step for assessing impact of future climate. *Science of the Total Environment* **511**, 562–575. https://doi.org/10.1016/j.scitotenv.2015.01.001.

Esteve, P., Varela-Ortega, C., Blanco-Gutiérrez, I. & Downing, T. E. 2015 A hydro-economic model for the assessment of climate change impacts and adaptation in irrigated agriculture. *Ecological Economics* **120**, 49–58. https://doi.org/10.1016/j.ecolecon.2015.09.017.

Faiz, M. A., Liu, D., Fu, Q., Li, M., Baig, F., Tahir, A. A., Khan, M. I., Li, T. & Cui, S. 2018 Performance evaluation of hydrological models using ensemble of General Circulation Models in the northeastern China. *Journal of Hydrology* **565**, 599–613. https://doi.org/10.1016/j.jhydrol.2018.08.057.

Fares, A., Bayabil, H. K., Zekri, M., Mattos, D. & Awal, R. 2017 Potential climate change impacts on citrus water requirement across major producing areas in the world. *Journal of Water and Climate Change* **8**, 576–592. https://doi.org/10.2166/wcc.2017.182.

Fenta Mekonnen, D. & Disse, M. 2018 Analyzing the future climate change of Upper Blue Nile River basin using statistical downscaling techniques. *Hydrology and Earth System Sciences* **22** (4), 2391–2408. https://doi.org/10.5194/hess-22-2391-2018.

Freedman, F. R., Pitts, K. L. & Bridger, A. F. C. 2014 Evaluation of CMIP climate model hydrological output for the Mississippi River Basin using GRACE satellite observations. *Journal of Hydrology* **519**, 3566–3577. https://doi.org/10.1016/j.jhydrol.2014.10.036.

Hamlat, A., Errih, M. & Guidoum, A. 2013 Simulation of water resources management scenarios in western Algeria watersheds using WEAP model. *Arabian Journal of Geosciences* **6** (7), 2225–2236. https://doi.org/10.1007/s12517-012-0539-0.

Han, D., Yan, D., Xu, X. & Gao, Y. U. 2017 Effects of climate change on spring wheat phenophase and water requirement in Heihe River basin, China. *Journal of Earth System Science* **126** (1), 16. https://doi.org/10.1007/s12040-016-0787-6.

Hassan, Z., Shamsudin, S. & Harun, S. 2014 Application of SDSM and LARS-WG for simulating and downscaling of rainfall and temperature. *Theoretical and Applied Climatology* **116** (1–2), 243–257. https://doi.org/10.1007/s00704-013-0951-8.

Höllermann, B., Giertz, S. & Diekkrüger, B. 2010 Benin 2025 – balancing future water availability and demand using the WEAP 'Water Evaluation and Planning' system. *Water Resources Management* **24** (13), 3591–3613. https://doi.org/10.1007/s11269-010-9622-z.

Hong, E., Nam, W.-H., Choi, J.-Y. & Pachepsky, Y. A. 2016 Projected irrigation requirements for upland crops using soil moisture model under climate change in South Korea. *Agricultural Water Management* **165**, 163–180. https://doi.org/10.1016/J.AGWAT.2015.12.003.

Hund, S. V., Allen, D. M., Morillas, L. & Johnson, M. S. 2018 Groundwater recharge indicator as tool for decision makers to increase socio-hydrological resilience to seasonal drought. *Journal of Hydrology* **563**, 1119–1134. https://doi.org/10.1016/j.jhydrol.2018.05.069.

Hussen, B., Mekonnen, A. & Pingale, S. M. 2018 Integrated water resources management under climate change scenarios in the sub-basin of Abaya-Chamo, Ethiopia. *Modeling Earth Systems and Environment* **4** (1), 221–240. https://doi.org/10.1007/s40808-018-0438-9.

Ishida, K., Ercan, A., Trinh, T., Jang, S., Kavvas, M. L., Ohara, N., Chen, Z. Q., Kure, S. & Dib, A. 2018 Trend analysis of watershed-scale annual and seasonal precipitation in Northern California based on dynamically downscaled future climate projections. *Journal of Water and Climate Change*. https://doi.org/10.2166/wcc.2018.241.

Jabloun, M. & Sahli, A. 2006 Development and comparative analysis of pedotransfer functions for predicting soil water characteristic content for Tunisian soil. In: *Proceedings of the 7th Edition of TIASSST*, Tunisia, pp. 170–178.

Jabloun, M. & Sahli, A. 2012 *WEAP-MABIA Tutorial: A Collection of Stand-Alone Chapters to aid in Learning the WEAP-MABIA Module*. Federal Institute for Geosciences and Natural Resources, Hannover, Germany. https://bit.ly/2lXl5Qp.

Karamouz, M., Ahmadi, A., Yazdi, M. S. S. & Ahmadi, B. 2013 Economic assessment of water resources management strategies. *Journal of Irrigation and Drainage Engineering* **140** (1), 1–13. https://doi.org/10.1061/(asce)ir.1943-4774.0000654.

Knezevic, M., Zivotic, L., Perovic, V., Topalovic, A. & Todorovic, M. 2017 Impact of climate change on olive growth suitability, water requirements and yield in Montenegro. *Italian Journal of Agrometeorology* **2**, 39–52. https://doi.org/10.19199/2017.2.2038-5625.039.

Lee, M. H. & Bae, D. H. 2016 Uncertainty assessment of future high and low flow projections according to climate downscaling and hydrological models. *Procedia Engineering* **154**, 617–623. https://doi.org/10.1016/j.proeng.2016.07.560.

Lespinas, F., Ludwig, W. & Heussner, S. 2014 Hydrological and climatic uncertainties associated with modeling the impact of climate change on water resources of small Mediterranean coastal rivers. *Journal of Hydrology* **511**, 403–422. https://doi.org/10.1016/j.jhydrol.2014.01.033.

Lhomme, J. P., Mougou, R. & Mansour, M. 2009 Potential impact of climate change on durum wheat cropping in Tunisia. *Climatic Change* **96**, 549–564. https://doi.org/10.1007/s10584-009-9571-9.

Lionello, P. & Scarascia, L. 2018 The relation between climate change in the Mediterranean region and global warming. *Regional Environmental Change* **18**, 1481–1493. https://doi.org/10.1007/s10113-018-1290-1.

Liu, D. L., O'Leary, G. J., Christy, B., Macadam, I., Wang, B., Anwar, M. R. & Weeks, A. 2017 Effects of different climate downscaling methods on the assessment of climate change impacts on wheat cropping systems. *Climatic Change* **144** (4), 687–701. https://doi.org/10.1007/s10584-017-2054-5.

Luo, X., Xia, J. & Yang, H. 2015 Modeling water requirements of major crops and their responses to climate change in the North China Plain. *Environmental Earth Sciences* **74**, 3531–3541. https://doi.org/10.1007/s12665-015-4400-0.

McNeill, S. J., Lilburne, L. R., Carrick, S., Webb, T. H. & Cuthill, T. 2018 Pedotransfer functions for the soil water characteristics of New Zealand soils using S-map information. *Geoderma* **326**, 96–110. https://doi.org/10.1016/j.geoderma.2018.04.011.

Milano, M., Ruelland, D., Dezetter, A., Fabre, J., Ardoin-Bardin, S. & Servat, E. 2013 Modeling the current and future capacity of water resources to meet water demands in the Ebro basin. *Journal of Hydrology* **500**, 114–126. https://doi.org/10.1016/j.jhydrol.2013.07.010.

Mouelhi, S., Michel, C., Perrin, C. & Andréassian, V. 2006 Stepwise development of a two-parameter monthly water balance model. *Journal of Hydrology* **318**, 200–214. https://doi.org/10.1016/j.jhydrol.2005.06.014.

Nash, J. E. & Sutcliffe, J. V. 1970 River flow forecasting through conceptual models part I – A discussion of principles. *Journal of Hydrology* **10**, 282–290. https://doi.org/10.1016/0022-1694(70)90255-6.

Nguyen, H., Mehrotra, R. & Sharma, A. 2017 Can the variability in precipitation simulations across GCMs be reduced through sensible bias correction? *Climate Dynamics* **49**, 3257–3275. https://doi.org/10.1007/s00382-016-3510-z.

Okkan, U. & Fistikoglu, O. 2014 Evaluating climate change effects on runoff by statistical downscaling and hydrological model GR2M. *Theoretical and Applied Climatology* **117** (1), 343–361. https://doi.org/10.1007/s00704-013-1005-y.

Okyereh, S. A., Ofosu, E. A. & Kabobah, A. T. 2019 Modelling the impact of Bui dam operations on downstream competing water uses. *Water-Energy Nexus* **2**, 1–9. https://doi.org/10.1016/j.wen.2019.03.001.

Olsson, T., Kämäräinen, M., Santos, D., Seitola, T., Tuomenvirta, H., Haavisto, R. & Lavado-Casimiro, W. 2017 Downscaling climate projections for the Peruvian coastal Chancay-Huaral Basin to support river discharge modeling with WEAP. *Journal of Hydrology: Regional Studies* **13**, 26–42. https://doi.org/10.1016/j.ejrh.2017.05.011.

Oudin, L., Perrin, C., Mathevet, T., Andréassian, V. & Michel, C. 2006 Impact of biased and randomly corrupted inputs on the efficiency and the parameters of watershed models. *Journal of Hydrology* **320** (2), 62–83. https://doi.org/10.1016/j.jhydrol.2005.07.016.

Ouyang, F., Zhu, Y., Fu, G., Lü, H., Zhang, A., Yu, Z. & Chen, X. 2015 Impacts of climate change under CMIP5 RCP scenarios on streamflow in the Huangnizhuang catchment. *Stochastic Environmental Research and Risk Assessment* **29** (7), 1781–1795. https://doi.org/10.1007/s00477-014-1018-9.

Pathak, T. B. & Stoddard, C. S. 2018 Climate change effects on the processing tomato growing season in California using growing degree day model. *Modeling Earth Systems and Environment* **4** (2), 765–775. https://doi.org/10.1007/s40808-018-0460-y.

Phan, T. T. H., Sunada, K., Oishi, S. & Sakamoto, Y. 2010 River discharge in the Kone River Basin (Central Vietnam) under climate change by applying the BTOPMC distributed hydrological model. *Journal of Water and Climate Change* **1** (4), 269–279. https://doi.org/10.2166/wcc.2010.046.

Psomas, A., Panagopoulos, Y., Konsta, D. & Mimikou, M. 2016 Designing water efficiency measures in a catchment in Greece using WEAP and SWAT models. *Procedia Engineering* **162**, 269–276. https://doi.org/10.1016/j.proeng.2016.11.058.

Rahmati, S. H., Nikakhtar, M. & Bavani, A. R. M. 2019 Impact of climate change on the future quality of surface waters: case study of the Ardak River, northeast of Iran. *Journal of Water and Climate Change* 1–18. https://doi.org/10.2166/wcc.2019.132.

Reshmidevi, T. V., Nagesh Kumar, D., Mehrotra, R. & Sharma, A. 2018 Estimation of the climate change impact on a catchment water balance using an ensemble of GCMs. *Journal of Hydrology* **556**, 1192–1204. https://doi.org/10.1016/J.JHYDROL.2017.02.016.

Rochdane, S., Reichert, B., Messouli, M., Babqiqi, A. & Khebiza, M. Y. 2012 Climate change impacts on water supply and demand in Rheraya watershed (Morocco), with potential adaptation strategies. *Water* **4**, 28–44. https://doi.org/10.3390/w4010028.

Rouhani, H. & Jafarzadeh, M. S. 2017 Assessing the climate change impact on hydrological response in the Gorganrood River Basin. *Iran. Journal of Water and Climate Change* **9** (3), 421–433. https://doi.org/10.2166/wcc.2017.207.

Rungee, J. & Kim, U. 2017 Long-term assessment of climate change impacts on Tennessee Valley Authority Reservoir operations: Norris Dam. *Water (Switzerland)* **9** (9). https://doi.org/10.3390/w9090649.

Saadi, S., Todorovic, M., Tanasijevic, L., Pereira, L. S., Pizzigalli, C. & Lionello, P. 2015 Climate change and Mediterranean agriculture: impacts on winter wheat and tomato crop evapotranspiration, irrigation requirements and yield. *Agricultural Water Management* **147**, 103–115. https://doi.org/10.1016/j.agwat.2014.05.008.

Salehnia, N., Hosseini, F., Farid, A., Kolsoumi, S., Zarrin, A. & Hasheminia, M. 2019 Comparing the performance of dynamical and statistical downscaling on historical run

precipitation data over a semi-arid region. *Asia-Pacific Journal of Atmospheric Sciences* 1–13. https://doi.org/10.1007/s13143-019-00112-1.

Schlenker, W., Hanemann, W. M. & Fisher, A. C. 2007 Water availability, degree days, and the potential impact of climate change on irrigated agriculture in California. *Climatic Change* **81** (1), 19–38. https://doi.org/10.1007/s10584-005-9008-z.

Sellami, H., Benabdallah, S., La, I. & Vanclooster, M. 2016 Quantifying hydrological responses of small Mediterranean catchments under climate change projections. *Science of the Total Environment* **543**, 924–936. https://doi.org/10.1016/j.scitotenv.2015.07.006.

Semenov, M. A. & Barrow, E. M. 2002 *LARS-WG A Stochastic Weather Generator for Use in Climate Impact Studies, Developed by Mikhail A. Semenov, Version 3.0 User Manual*. Retrieved from http://www.iacr.bbsrc.ac.uk/mas-models/larswg.html.

Semenov, M. A. & Stratonovitch, P. 2015 Adapting wheat ideotypes for climate change: accounting for uncertainties in CMIP5 climate projections. *Climate Research* **65**, 123–139. https://doi.org/10.3354/cr01297.

Semenov, M. A., Brooks, R. J., Barrow, E. M. & Richardson, C. W. 1998 Comparison of the WGEN and LARS-WG stochastic weather generators for diverse climates. *Climate Research* **10** (2), 95–107. https://doi.org/10.3354/cr010095.

Teutschbein, C. & Seibert, J. 2012 Bias correction of regional climate model simulations for hydrological climate-change impact studies: review and evaluation of different methods. *Journal of Hydrology* **456–457**, 12–29. https://doi.org/10.1016/j.jhydrol.2012.05.052.

Todorovic, A. & Plavsic, J. 2016 The role of conceptual hydrologic model calibration in climate change impact on water resources assessment. *Journal of Water and Climate Change* **7** (1), 16–28. https://doi.org/10.2166/wcc.2015.086.

Van Engelen, V., Batjes, N. & Huting, J. 2005 *Harmonized Global Soil Resources Database*. Report 2005/06, ISRIC – World Soil Information and Food and Agriculture Organization of the United States, Wageningen, The Netherlands.

Varela-Ortega, C., Blanco-Gutiérrez, I., Esteve, P., Bharwani, S., Fronzek, S. & Downing, T. E. 2016 How can irrigated agriculture adapt to climate change? insights from the Guadiana Basin in Spain. *Regional Environmental Change* **16** (1), 59–70. https://doi.org/10.1007/s10113-014-0720-y.

Wang, X., Zhang, J., Ali, M., Shahid, S., He, R., Xia, X. & Jiang, Z. 2016 Impact of climate change on regional irrigation water demand in Baojixia irrigation district of China. *Mitigation and Adaptation Strategies for Global Change* **21**, 233–247. https://doi.org/10.1007/s11027-014-9594-z.

Yates, D., Purkey, D., Sieber, J., Huber-Lee, A. & Galbraith, H. 2005a Planning model part 2: aiding freshwater ecosystem service evaluation. *Water International* **30** (4), 501–512.

Yates, D., Sieber, J., Purkey, D. & Huber-Lee, A. 2005b International water resources association WEAP21 – A demand-, priority-, and preference-driven water planning model part 1: model characteristics. *Water International* **30** (4), 487–500.

Zamani, R., Akhond-Ali, A. M., Roozbahani, A. & Fattahi, R. 2017 Risk assessment of agricultural water requirement based on a multi-model ensemble framework, southwest of Iran. *Theoretical and Applied Climatology* **129** (3–4), 1109–1121. https://doi.org/10.1007/s00704-016-1835-5.

Zeroual, A., Meddi, M. & Bensaad, S. 2013 The impact of climate change on river flow in arid and semi-arid rivers in Algeria. *IAHS-AISH Proceedings and Reports* **359** (July), 1–6.

Zeroual, A., Assani, A. A., Meddi, M. & Alkama, R. 2019 Assessment of climate change in Algeria from 1951 to 2098 using the Köppen–Geiger climate classification scheme. *Climate Dynamics* **52**, 227–243. https://doi.org/10.1007/s00382-018-4128-0.

Zheng, H., Chiew, F. H. S., Charles, S. & Podger, G. 2018 Future climate and runoff projections across South Asia from CMIP5 global climate models and hydrological modelling. *Journal of Hydrology: Regional Studies* **18**, 92–109. https://doi.org/10.1016/j.ejrh.2018.06.004.

Zhou, T., Wu, P., Sun, S., Li, X., Wang, Y. & Luan, X. 2017 Impact of future climate change on regional crop water requirement-A case study of Hetao irrigation district, China. *Water (Switzerland)* **9** (6). https://doi.org/10.3390/w9060429.

First received 7 July 2019; accepted in revised form 9 October 2019. Available online 5 December 2019